Pergamon

Int. J. Solids Structures Vol. 33, No. 7, pp. 1053–1068, 1996

0020-7683/96 $15.00 + .00

0020-7683(95)00088-7

COMMENTS ON THE MROZ MULTIPLE SURFACE TYPE PLASTICITY MODELS

YANYAO JIANG and HUSEYIN SEHITOGLU
Department of Mechanical and Industrial Engineering, University of Illinois at Urbana-Champaign, 1206 West Green Street, Urbana, IL61801, U.S.A.

(*Received* 26 *January* 1994; *in revised form* 30 *March* 1995)

Abstract Several questions are addressed regarding the role of number of surfaces in the Mroz type multiple surface models. Firstly, increasing the number of surfaces improves the accuracy of the plastic modulus function, but at the same time alters the translation behavior of surfaces. Two 90° out-of-phase axial–torsion loading experiments are chosen to illustrate the number of surface influence on the model behavior. The stresses exceed the experimental levels with increasing numbers of surfaces from 5 to 100. Secondly, for proportional loading, the multiple surface models do not predict ratchetting (progressive plastic strain accumulation in one direction). However, these models predict ratchetting for general nonproportional loading. An "ellipse" shaped axial–torsional loading path has been considered where predicted ratchetting rates far exceeded their experimental counterparts. An explanation is forwarded to address these properties of the models. It is further demonstrated that the multiple surface model of Mroz and its modification by Garud produce identical stress–strain predictions when the number of surfaces exceeds a certain value. For infinitesimal loading increment, intersection of surfaces does not occur when using either the Mroz or Garud model, however, when finite loading increment is selected in numerical calculations the intersection problem arises in the Mroz model.

NOMENCLATURE

f	yield surface function
$f_{(i)}$	a surface in a multiple surface model
h	plastic modulus function
k	yield stress in simple shear
$\underline{\mathbf{n}}$	unit exterior normal to the yield surface at the stress state
N	number of loading cycles
N_s	number of surfaces employed in a multiple surface model
p	equivalent plastic strain
$R_{(i)}$	radius of the ith surface in the Mroz multiple surface type hardening rules
$\underline{\mathbf{S}}$	deviatoric stress tensor
$\underline{\alpha}$	total backstress tensor
$\underline{\alpha}^{(i)}$	center of the ith surface in deviatoric stress space for the multiple surface models
Δ	prefix denoting range
$\underline{\varepsilon}^p$	plastic strain tensor
$\underline{\varepsilon}$	total strain tensor
$\underline{\sigma}$	stress tensor
$\underline{\gamma}$	Mroz translation vector
$\underline{\gamma}'$	Garud translation vector

1. INTRODUCTION

The multiple surface models forwarded by Mroz (1967, 1969) and later by Garud (1981) have gained wide appeal in the cyclic plasticity research over the last 20 years. An obvious advantage of the multiple surface models is their ability to reproduce the Bauschinger effect for Masing type materials. The Bauschinger effect refers to the phenomenon that the yield stress will be reduced in one direction if the material has been loaded plastically in the opposite direction. The material is said to conform to Masing behavior when the cyclic stress–strain curve, obtained by joining the tips of the hysteresis loops for different strain amplitudes, reproduces the hysteresis loop shape corresponding to each strain amplitude. The multiple surface models are also noteworthy for their capabilities for handling additional hardening for nonproportional loading. It has been demonstrated that this class of models can correlate experiments better than the linear hardening model when predicting

the stress responses for multiaxial strain-controlled loading (Hunsaker *et al.*, 1976; Lamba and Sidebottom, 1978). The superiority of the multiple surface models is also reflected in the overwhelming efforts on developing the simplified two-surface models (e.g., Dafalias and Popov, 1975; Krieg, 1975; McDowell, 1985; Tseng and Lee, 1983) and three-surface models (Bruhns and Pape, 1989; Chaboche, 1989). Attempts have also been made to advance the computational schemes associated with the Mroz multiple surface model (Chu, 1984; Kottgen and Seeger, 1993). The multiple surface models have been applied to engineering problems (Barkey *et al.*, 1994; Chu, 1984; Garud, 1991; Howell *et al.*, 1993) and the encouraging simulations reported in the literature suggest that the multiple surface models are able to provide stress–strain responses in close agreement with the experimental observations for general nonproportional loading.

In spite of many advantages, there are certain concerns associated with the multiple surface models. The discontinuous description of plastic modulus function may leave a continuity condition unfulfilled (Hashiguchi, 1993). If the sizes of the surfaces are allowed to vary, certain conditions should be satisfied to avoid intersection of surfaces. Therefore, it is difficult to incorporate the transient material behavior such as isotropic hardening and cyclic hardening into the multiple surface models (excluding the two and three surface models). With the uniaxial stress–strain curve as the only input, the models do not have sufficient flexibility to predict different levels of nonproportional hardening experimentally confirmed for different materials. Furthermore, the multiple surface models do not predict ratchetting, plastic strain accumulation in a given direction, for any proportional loading, but they are able to predict ratchetting for general nonproportional loading (Garud, 1991; Hassan *et al.*, 1992; Jiang, 1993). Hassan *et al.* (1992) and Jiang (1993) showed that the predicted ratchetting rate obtained by using the Mroz model was much higher than the experimental observations. It has not been fully understood why multiple surface models produce ratchetting for nonproportional loading but zero ratchetting for proportional loading. The present study addresses this concern.

Hashiguchi (1988) formulated the conditions for multiple surfaces to intersect for the Mroz hardening rule and pointed out that surface intersection would occur. McDowell (1989) discussed the intersection problem for the two-surface models and concluded that a two-surface model following the Mroz translation direction posed no surface intersection problem. The current work will further address this intersection issue for the multiple surface models. It was noted that the number of surfaces employed in a multiple surface model has an influence on the surface translation (Kottgen and Seeger, 1993). In this paper the number of surfaces influenced will be elucidated to predict ratchetting for non-proportional loading.

In the following discussions, the structure of the Mroz and Garud multiple surface models will be introduced along with the basic framework of time-independent plasticity theory. We will restrict the discussion to the conventional representation of plasticity (Drucker, 1988), which assumes that no plastic deformation will occur in the elastic region of yield surface. Distinction will be made between two or three-surface models and multiple-surface models. In the remainder of the paper, emphasis will placed on the multiple-surface models. Specifically, we will discuss the number of surface influence on the stress–strain simulations and ratchetting prediction problems in general.

2. STRUCTURE OF MULTIPLE SURFACE PLASTICITY MODELS

Under the well-established framework of plasticity theories, for small deformations the total strain is decomposed into the elastic and plastic parts. The elastic part is governed by Hook's law and the plastic part is the subject of plasticity theories. For plastic deformation, the incompressibility condition is generally assumed. The material follows the elastic stress–strain relation with zero plastic strains until the stresses satisfy the yield condition. The von Mises yield function and the normality flow rule are used for the purpose of discussions.

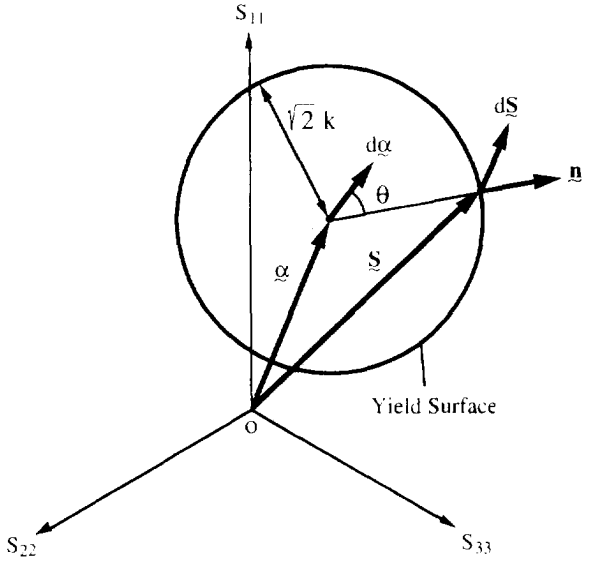

Fig. 1. Generalized von Mises yield surface with kinematic translation in deviatoric stress space.

$$f = (\underset{\sim}{S} - \underset{\sim}{\alpha}) : (\underset{\sim}{S} - \underset{\sim}{\alpha}) - 2k^2 = 0, \tag{1}$$

$$d\underset{\sim}{\varepsilon}^p = \frac{1}{h} \langle d\underset{\sim}{S} : \underset{\sim}{n} \rangle \underset{\sim}{n}. \tag{2}$$

A bold letter with a tilde below represents a second order Cartesian tensor. In eqn (1), f represents a yield surface, $\underset{\sim}{S}$ is the deviatoric stress tensor, $\underset{\sim}{\alpha}$ is the backstress in deviatoric space representing the center of the yield surface, and k is the yield stress in simple shear. In eqn (2), $\langle\rangle$ denotes the MacCauley bracket (i.e. $\langle x \rangle = 0.5\ (x + |x|)$) and h is a scalar function often called the plastic modulus function. A colon between two tensors denotes their inner product and the prefix d represents infinitesimal increment or differentiation. A schematic representation of the yield surface and its translation is illustrated in Fig. 1. The angle between the back stress translation and the exterior normal is denoted by θ. The unit exterior normal $\underset{\sim}{n}$ on the yield surface at the loading point is defined as,

$$\underset{\sim}{n} = \frac{\underset{\sim}{S} - \underset{\sim}{\alpha}}{|\underset{\sim}{S} - \underset{\sim}{\alpha}|} \tag{3}$$

The shape of the yield surface is generally assumed unchanged; however, the size of the yield surface can be adapted to account for the transient behavior by allowing k to vary. It is also assumed that the yield surface can translate but cannot rotate.

During elastic–plastic deformation the stress state lies on the yield surface. This consistency condition can be expressed mathematically as

$$df = 0, \tag{4a}$$

or modifying eqn (1),

$$d\underset{\sim}{S} : \underset{\sim}{n} - d\underset{\sim}{\alpha} : \underset{\sim}{n} - 2\,dk = 0. \tag{4b}$$

To model the observed stress–strain response of a material under cyclic loading, Mroz (1967, 1969) introduced the concept of a field of plastic moduli. Several points are selected

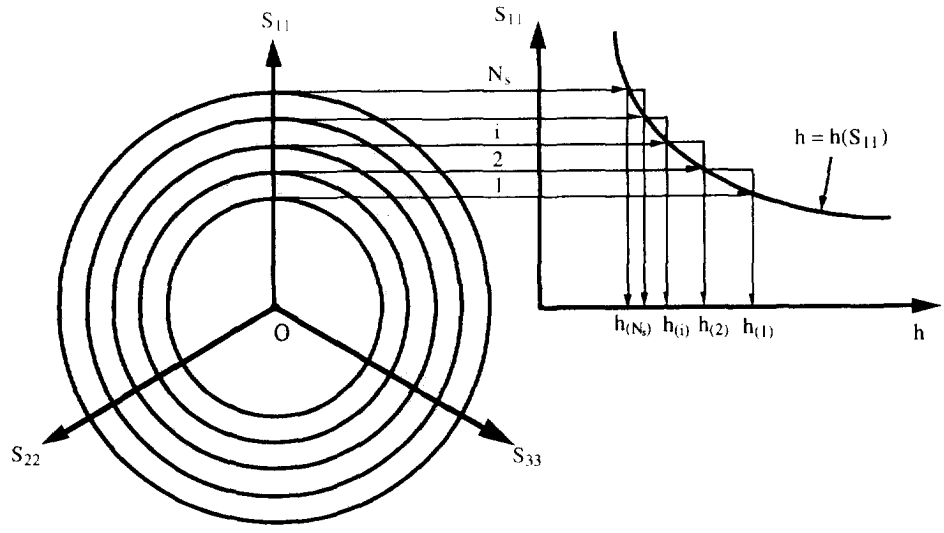

Fig. 2. Field of constant plastic modulus functions.

on the uniaxial stress–strain curve (refer to Fig. 2), and corresponding to each point, a surface in the stress space is defined to be geometrically similar to the initial yield surface. Mroz postulated that these surfaces define regions in the stress space, each having a constant plastic modulus function, $h(1)$, $h(2)$, $h(i)$, $h(N_s)$ where N_s is the number of the outermost surface. Independently, Iwan (1967) proposed a similar multiple surface model to consider the Bauschinger effect for Masing type materials.

Mroz (1967) proposed that the translation direction of a surface is given by the vector joining the present state of stress P on the ith surface with the image stress state P^* on the $(i+1)$th surface such that the two surfaces have an identical exterior normal $\underline{\mathbf{n}}$ (see Fig. 3). This Mroz translation vector can be expressed as

$$\underset{\sim}{\nu} = (R_{(i+1)} - R_{(i)})\underline{\mathbf{n}} + \underset{\sim}{\alpha}^{(i+1)} - \underset{\sim}{\alpha}^{(i)}, \tag{5}$$

where $\underset{\sim}{\alpha}^{(i)}$ and $R_{(i)}$ represent the center and radius of the ith surface, respectively. The

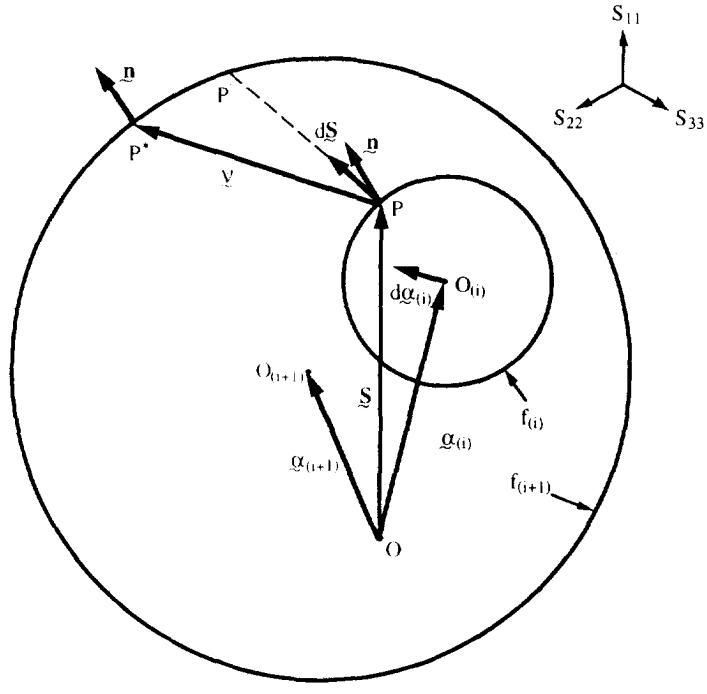

Fig. 3. Schematic of the Mroz hardening rule illustrating translation direction.

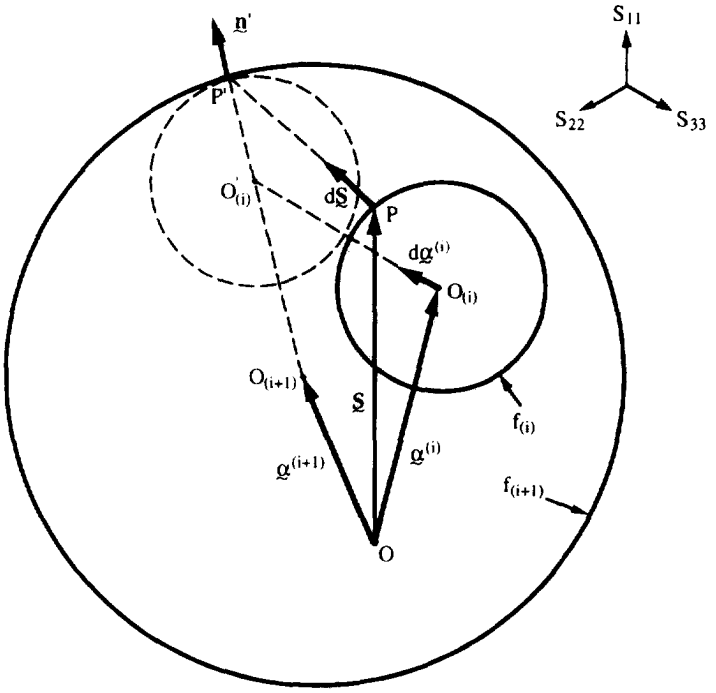

Fig. 4. Schematic of the Garud hardening rule illustrating translation direction.

increment of the ith surface center is determined by manipulating eqn (5) and the consistency condition, eqn (4). The first surface $f_{(1)}$ is the yield surface and any other surface represents constant plastic modulus functions.

Garud (1981), in examining hardening rules, pointed out that the translation direction of the yield surface, according to both the Mroz and Prager–Ziegler (Prager, 1955; Ziegler, 1959) rules, was independent of the stress increment, and this independence would create an inconsistency problem in the finite stress increment calculation. To avoid this possible inconsistency, Garud proposed a new hardening rule that related the surface translation direction to the stress increment direction. Referring to Fig. 4, consider that the stress increment was so large that it joined the current stress state point P on the ith surface and P' on the $(i+1)$th surface, so that the two surfaces would be tangential on point P' where the ith surface had its center on O_i'. Garud proposed that the translation direction of the ith surface is in the direction of the vector joining O_i and O_i', and the magnitude of translation is determined by a consistency condition which requires that a stress state stay on the yield surface. Therefore, the Garud translation vector, the vector joining point O_i and O_i', can be expressed as

$$\underset{\sim}{y}' = (R_{(i+1)} - R_{(i)})\underline{\mathbf{n}}' + \underset{\sim}{\alpha}_{(i+1)} - \underset{\sim}{\alpha}_{(i)}, \tag{6}$$

where $\underline{\mathbf{n}}'$ is the unit exterior normal at point P' which is often called the incremented stress state. Other than the prime notation, both sets of equations for the Mroz and Garud translation directions are similar. Clearly the only difference between the Garud rule and the Mroz rule is that the translation direction in the Mroz rule is determined by the normal $\underline{\mathbf{n}}$ of the current stress state, while in the Garud rule the translation direction is determined by the normal $\underline{\mathbf{n}}'$ of the incremented stress state. The magnitude of translation of a surface for the Mroz model is determined by

$$\mathrm{d}\underset{\sim}{\alpha}^{(i)} = \frac{\mathrm{d}\underset{\sim}{S} : \underline{\mathbf{n}}}{\underset{\sim}{y} : \underline{\mathbf{n}}}\,\underset{\sim}{y}.$$

For the Garud model, $\underset{\sim}{y}$ is replaced by $\underset{\sim}{y}'$ in the previous expression. The magnitudes and directions of translations for the two models are different.

Primarily aimed at reducing the computational time, the two-surface plasticity models, consisting of a yield surface and a bounding surface, were developed based on the concept that the translation direction of the yield surface is determined by the relative positions of the two surfaces. The translation of the yield surface follows either the Mroz hardening rule (Dafalias, 1981; Dafalias and Popov, 1975; Krieg, 1975) or Garud hardening rule (Tseng and Lee, 1983).

It should be noted that the two-surface models differ from the multiple surface models of Mroz and Garud in the way they specify the plastic modulus functions. For proportional loading, the Mroz–Garud models predict fully closed stress–strain hysteresis loops, hence no ratchetting; while the two-surface models with a nonlinear hardening relationship can produce ratchetting for both proportional and nonproportional loadings (McDowell, 1992). Mroz (1981, 1983) discussed the similarity between the multiple surface models and the Armstrong–Frederick type single surface models. Ohno and Wang (1991) further formalized the relationship between the multiple surface models and the single surface formulations.

Preliminary analysis (Jiang, 1993) suggests that the Mroz and Garud multiple surface models are inferior to the Armstrong–Frederick (Armstrong and Frederick, 1966) type models such as those of Chaboche *et al.* (1979) and Ohno and Wang (1993) not only in the ratchetting prediction but also in the stress response predictions for nonproportional strain-controlled loading. Therefore, we draw a distinction between the multiple surface models of Mroz and Garud and the single and the two-surface models. We will concentrate our discussion to the multiple surface models.

3. INTERSECTION OF SURFACES

In discussing Mroz–Garud multiple surface relations, it has been always taken for granted that (i) the surfaces remain tangential on the point of stress state and (ii) in the course of translation the surfaces will never intersect. In fact, when the point of stress state is always the point of tangency of the surfaces, there will be no possibility for the surfaces to intersect. Here, we demonstrate that this is true for an infinitesimal loading increment. Figure 5 depicts a critical position before possible interaction could occur. Without loss of generality, discussion will be restricted to two neighboring surfaces, $f_{(i)}$ and $f_{(i+1)}$. Assume that at the current moment the two surfaces are tangential at point T and the stress state is at point P on the ith surface. The exterior normal at point P is $\underline{n}$. The image point in the

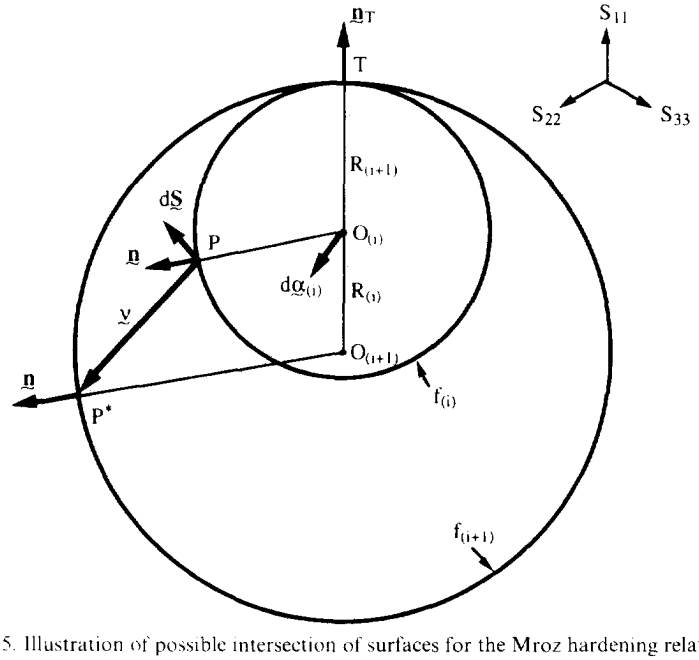

Fig. 5. Illustration of possible intersection of surfaces for the Mroz hardening relation.

$(i+1)$th surface which has an identical exterior normal $\underline{\mathbf{n}}$ is P^*. According to the Mroz hardening relation, the translation of ith surface should follow the vector joining point P and point P^*, i.e. $\underline{v}$. Simplifying the Mroz translation vector represented by eqn (5) for the Fig. 5 situation results in

$$\underline{v} = (R_{(i+1)} - R_{(i)})\underline{\mathbf{n}} + \underline{z}^{(i+1)} - \underline{z}^{(i)} = (R_{(i+1)} - R_{(i)})(\underline{\mathbf{n}} - \underline{\mathbf{n}}_T), \tag{7}$$

where $\underline{\mathbf{n}}_T$ is the unit exterior normal at point T where the ith surface touches the $(i+1)$th surface. $R_{(i)}$ and $R_{(i+1)}$ denote the radii of the ith and $(i+1)$th surfaces, respectively. Because $(R_{(i+1)} - R_{(i)}) > 0$ and noting that both $\underline{\mathbf{n}}$ and $\underline{\mathbf{n}}_T$ are unit vectors, from eqn (7) we have

$$\underline{v} \cdot \underline{\mathbf{n}}_T = (R_{(i+1)} - R_{(i)})(\underline{\mathbf{n}} \cdot \underline{\mathbf{n}}_T - 1) < 0. \tag{8}$$

The equal sign in the previous inequality holds only when the loading state point P coincides with point T. In this case the two surfaces, $f_{(i)}$ and $f_{(i+1)}$, will translate in a direction determined by the relative position of $(i+2)$th surface in terms of $f_{(i+1)}$ or $f_{(i)}$, which is not the case under consideration. Noting that the direction of $\mathrm{d}\underline{z}^{(i)}$ is parallel to $\underline{v}$, the inequality implies that whenever the stress point is at a point other than point T the translation direction of the ith surface always makes an obtuse angle to the exterior normal $\underline{\mathbf{n}}_T$ at point T where the ith and $(i+1)$th surfaces were tangential. Therefore, the ith surface will depart from the initially tangential point T as a result of further loading. This condition suggests that when two surfaces are tangential at a point other than the stress point, further loading will force those two surface to separate. When the loading point P reaches the $(i+1)$th surface, the two surface will be tangential at a point and, according to the aforementioned condition, this point should be the loading point P. This confirms the previous assertion that the surfaces will be tangential on the point of stress state and the surfaces will never intersect. Upon replacing $\underline{\mathbf{n}}$ in eqn (8) with $\underline{\mathbf{n}}'$, the exterior unit normal at the incremented stress state, we can reach the same conclusions for the Garud model.

From the previous discussions on the Mroz model, we conclude that when the loading path follows PP' in Fig. 3, the ith surface will be tangent to the $(i+1)$th surface at point P'. On the other hand in Fig. 4 for the Garud rule, the ith and $(i+1)$th surfaces will be also tangential at point P' on the $(i+1)$th surface when the loading point P reaches P'. Clearly, the resulting translation of the ith surface will be the same according to both the Mroz and Garud rules when the number of surfaces is increased. This will be demonstrated and further discussed.

The previous discussion of the intersection problem assumes that the stress increment is infinitesimal. Note that the term infinitesimal here is a mathematical terminology. Because the translation direction of a surface is independent of the stress increment, surface intersection may occur for the Mroz model when the stress increment is finite. A simple example is illustrated in Fig. 6. When the current stress point P lies in the extended line linking $O_{(i)}$ and $O_{(i+1)}$, the current centers of the ith and $(i+1)$th surfaces, respectively, the translation of the ith surface should be consistent with the exterior normal direction on the ith surface at point P. A finite stress increment $\Delta\underline{\mathbf{S}}$ perpendicular to the normal direction, $\underline{\mathbf{n}}$, in deviatoric stress space from P to P^* will result in intersection of the two surfaces. However, such intersection problem does not exist for the Garud model, even for finite stress increment. Referring to Fig. 4, the Garud rule requires that the two surfaces, $f_{(i)}$ and $f_{(i+1)}$, be tangential at the point P' when the loading stress state reaches the $(i+1)$th surface. We established that there is no intersection problem for infinitesimal stress increment. Therefore, the surface intersection problem can be circumvented in the numerical analysis when using the Mroz model by systematically refining the loading increment step. In the numerical analysis where finite loading increment is utilized, measures such as those described by Tipton (1985) should be also taken for the case when a loading step crosses a surface.

We note that the current conclusion on the surface intersection contrasts to that of Hashiguchi (1988) who concluded that the surfaces may intersect for the Mroz model. McDowell (1989) also pointed out that a two-surface model obeying the Garud translation

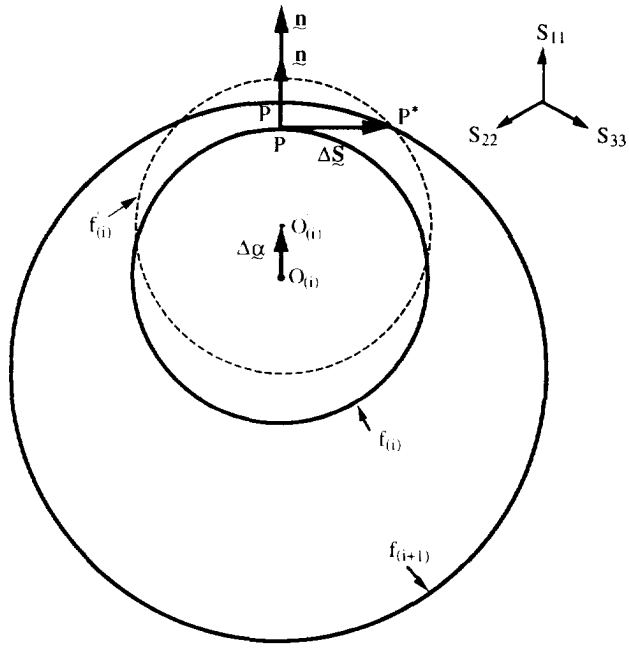

Fig. 6. Intersection of surfaces when employing the Mroz model for finite stress increment.

direction had a region where the boundary surface and the yield surface would intersect, but there was no intersection problem if the yield surface follows the Mroz translation direction. In some of the two-surface models, the bounding surface is allowed to translate *independently* (McDowell, 1989), even it is not "touched" by the yield surface. This independence of translation of the bounding surface may result in surface intersection. This difference contributed to miscellaneous conclusions concerning the intersection problem in the literature.

4. NUMBER OF SURFACE INFLUENCE ON STRESS–STRAIN PREDICTIONS

The plastic modulus function is described with the piecewise linear representation in the multiple surface models. Inevitably, the number of surfaces employed in the model has an influence on the description of the stress–strain relations for a proportional loading. For uniaxial loading the piecewise linear description in the multiple surface models will approach the experimental stress–strain curve as increasing number of surfaces are employed. On the other hand, the translation direction of a surface is dependent on the relative positions of the consecutive surfaces. Therefore, it becomes evident that the number of surfaces employed also has an influence on the surface translations. For discussion, we consider only the cyclically stable material. When the yield stress is a constant, eqn (4b) renders

$$d\underline{S} : \underline{n} = d\underline{\alpha} : \underline{n}. \tag{9}$$

Substituting the above relation into eqn (2), we obtain

$$d\underline{\varepsilon}^p = \frac{1}{h}(d\underline{\alpha} : \underline{n})\underline{n} = \frac{1}{h}|d\underline{\alpha}| \cos\theta \underline{n}, \tag{10}$$

where θ is the angle made by the exterior normal direction $\underline{n}$ and the translation direction of the yield surface (refer to Fig. 1) in deviatoric stress space. The quantity $|d\underline{\alpha}|$ in eqn (10) is the magnitude of the backstress increment which is defined as $|d\underline{\alpha}| = \sqrt{d\underline{\alpha} : d\underline{\alpha}}$. With the other conditions being the same for a stress-controlled loading path, eqn (10) implies that the larger the angle θ the smaller the corresponding plastic deformation predicted. If the

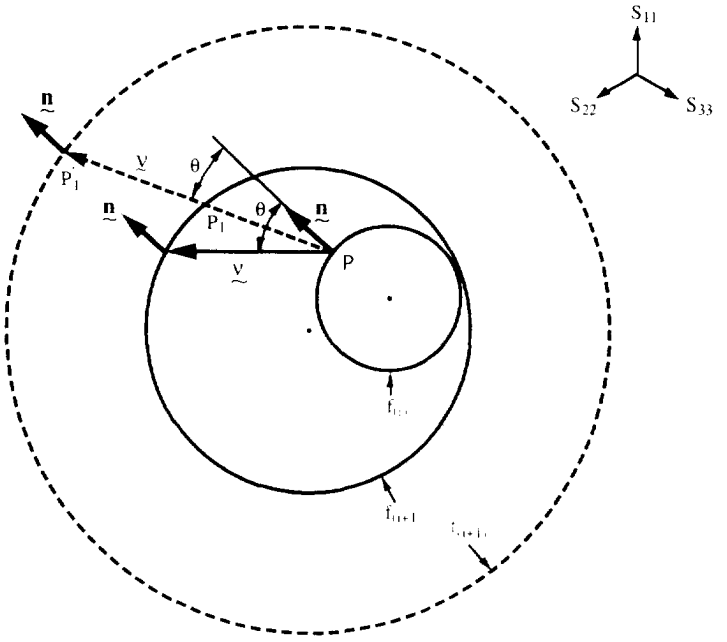

Fig. 7. Illustration of the number of surface influence on the translation of a surface.

strains are controlled parameters, eqn (10) suggests that a larger angle θ will result in a larger stress response. In the case of stress-controlled loading (where stress increments are known beforehand and plastic strains are to be computed) consider two cases with the same number of selected surfaces and plastic modulus functions. The one with a larger angle θ will result in smaller plastic deformation. Importantly, the angle θ can be viewed as a measure of nonproportionality effects (Benallal and Marquis, 1987). We find that the number of surfaces not only influences h, as noted by other investigators, but influences θ considerably. The relationship between ratchetting and θ was discussed by Jiang and Sehitoglu in a recent paper (Jiang and Sehitoglu, 1994).

Figure 7 schematically illustrates the number of surface influence on the translation direction of a surface when using the Mroz multiple surface model. Considering the case when the $1-i$th surfaces are tangential at the loading point P and the next neighboring surface is $f_{(i+1)}$, the translation direction of the ith surface will follow the direction $\underset{\sim}{v}$ and the corresponding angle between the normal $\underset{\sim}{n}$ and the translation direction $\underset{\sim}{v}$ is θ. If the number of surfaces is reduced so that the next neighboring surface size should become larger, the translation direction of the ith surface would follow $\underset{\sim}{v}'$ direction that makes an angle θ' with $\underset{\sim}{n}$. Accordingly, for the same stress loading path, the predicted results will be different if employing a different number of surfaces. The number of surface influence on the Garud translation direction can be explained in the same fashion.

4.1. *Nonproportional loading experiments under strain control*

Two strain-controlled 90° out-of-phase axial-torsion loading paths are investigated. The experimental data is obtained from Fatemi (1985) who conducted his experiments on the same equipment as the authors at the University of Illinois. Two loading paths are shown in Fig. 8. The uniaxial stress–strain curves used in the simulations are shown in Fig. 9 for different number of surfaces selected. The yield stress is 173 MPa. The largest surface corresponds to a uniaxial stress of 700 MPa. The surfaces in between the yield surface and the largest surface are evenly spaced. Figure 9 shows that the number of surfaces employed has little effect on the uniaxial stress–strain relation when the number of surfaces is larger than five. The effect of the number of surface influence under proportional loading is small and converges asymptotically.

Figure 10(a) shows results predicted by the Mroz model for path I. Little influence of the number of surfaces is noted. However, the number of surfaces has a profound effect on

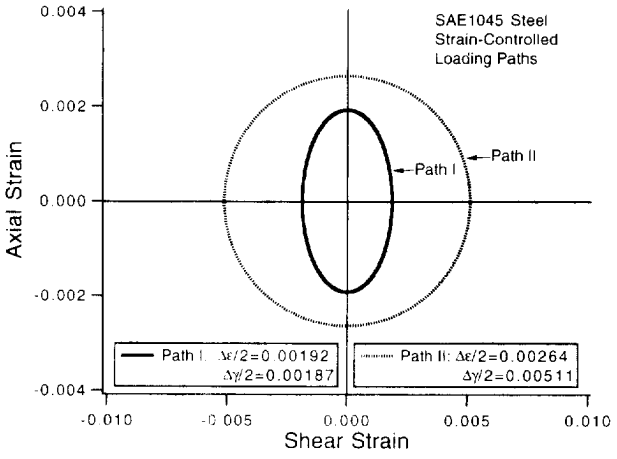

Fig. 8. Strain-controlled loading paths (1045 steel).

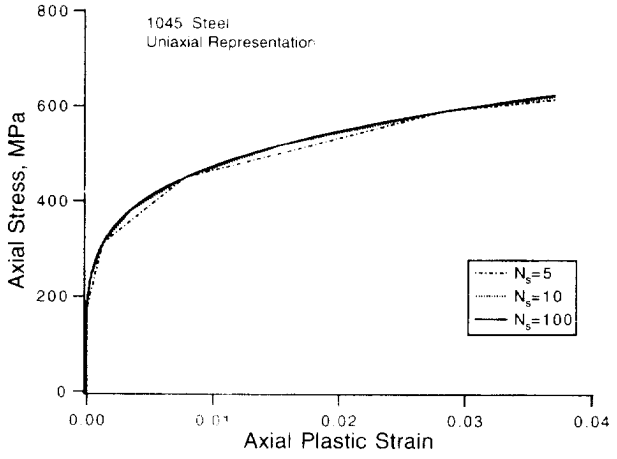

Fig. 9. Uniaxial representation for 1045 steel with different number of surfaces.

the predictions of the stress response for path II (Fig. 10b) when using the Mroz model. When the number of surface is five, the predicted stress response is in close agreement with the experimental data. When the number of surfaces is increased, higher stress responses are predicted. Similar phenomenon can be observed for the Garud model. For path I, the Garud model is insensitive to the selection of the number of surface. However, the number of surface influence becomes significant for path II when using the Garud model (Fig. 11). Of all the selections of the number of surfaces, the Garud model does not give results in good agreement with the experiment. It is noted that when N_s is larger than 50, the two models predict very similar results for the two loading paths investigated.

To illustrate this point further we consider 1070 steel (Fig. 12a) subjected to a strain-controlled 90° out-of-phase tension torsion experiment (Fig. 12b) to demonstrate this effect. Assume that the material obeys a bilinear stress–strain relation for uniaxial loading (Fig. 12a). The purpose of this choice is to isolate the number of surface effect on the translation of the surfaces. For this material, the material constants for the multiple surface models include the Young's modulus, E, the yield stress, σ_y, the plastic modulus, H, and the Poisson's ratio, μ. These material properties are presented in Fig. 12a. It should be noted that the selection of the material constants does not qualitatively alter the ensuing points of discussion.

The predictions obtained using the Mroz and Garud models with different number of surfaces are shown in Fig. 12b. The experimental strain path is depicted in the upper-right corner of Fig. 12b. N_s in the figure denotes the number of surfaces employed when using the Mroz or Garud model. There are 4000 incremental steps used for a loading cycle in the

(a)

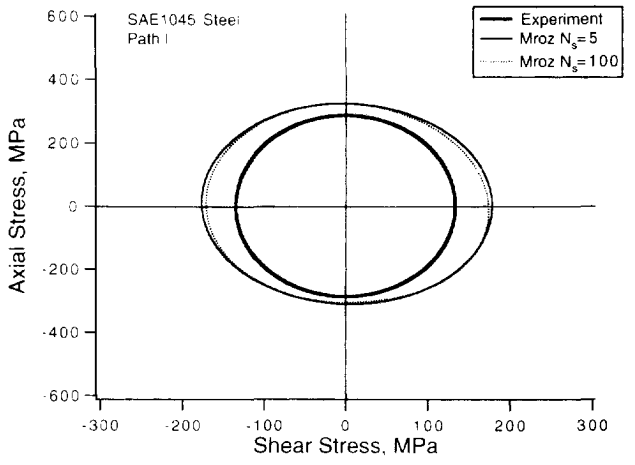

(b)

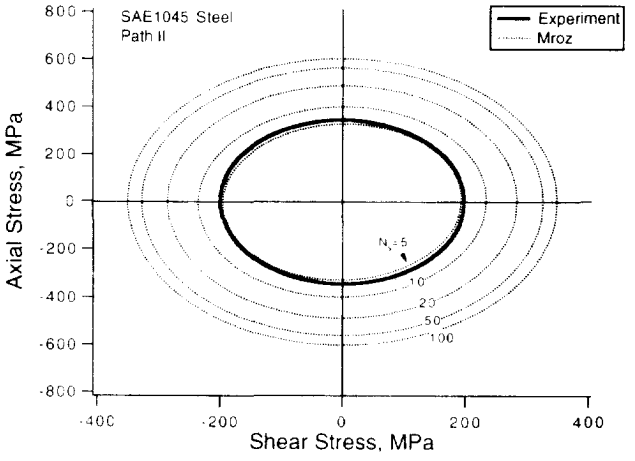

Fig. 10. Comparison of experimental data and the Mroz predictions: (a) stress response (path I); (b) stress response (path II).

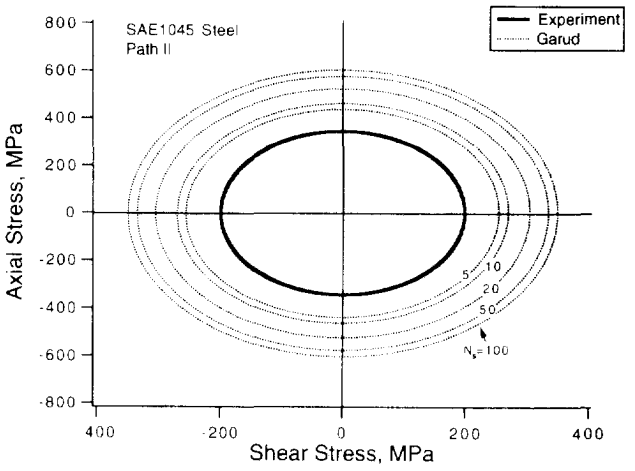

Fig. 11. Comparison of experimental data and the Garud predictions.

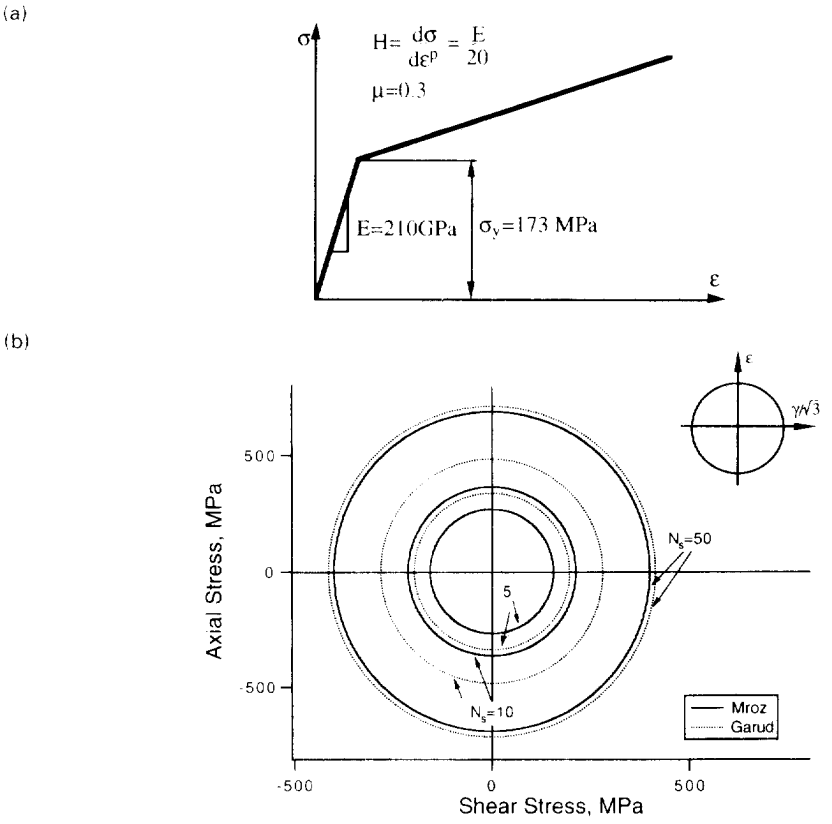

Fig. 12. Demonstration of the number of surface influence on the Mroz and Garud predictions: (a) bilinear stress–strain representation and material constants used in the Mroz and Garud simulations; (b) stress responses predicted by the Mroz and Garud models for a strain-controlled nonproportional tension–torsion loading path.

simulations. The largest surface in the multiple surface models corresponds to about 10% strain amplitude for the uniaxial loading and the surfaces in between the largest surface and the smallest (yield) surface are uniformly distributed in deviatoric stress space. From Fig. 12b we recognize the significant influence of the number of surfaces on the stress response predictions. For the 90° out-of-phase loading path, the Mroz and Garud models predict higher stresses as the number of surface increases.

We note that with bilinear stress–strain representation for uniaxial loading, all the values of the plastic modulus functions represented by each surface in the models are identical. In other words, there is no influence of the number of surface on the plastic modulus function. Therefore, all the deviation shown in Fig. 12b is attributed to the alteration of translation direction of the yield surface due to employing different number of surfaces. Also, we observe that both multiple surface models predict practically the same results when $N_s = 50$. This is consistent with the previous discussion of the Mroz and Garud models. From the numerical analyses employing the multiple surface models, it has been noted that the seriousness of the number of surface influence is also dependent on the loading magnitude and loading path (Jiang, 1993).

For general applications of the multiple surface models, the number of surfaces cannot be very large due to the limitation of the computational ability. The tremendous influence of the number of surfaces, as shown in Figs 9–12, reveals an important controversy of the multiple surface models. A hardening rule is identified by its unique specification of the translation direction for the yield surface. In the multiple surface models, however, the number of surfaces employed becomes an important model parameter for this specification. The quantitative relation between the number of surfaces and the predicted results is difficult to formulate. Many existing conclusions related to the multiple surface models should be reviewed in the context of the number of surfaces employed.

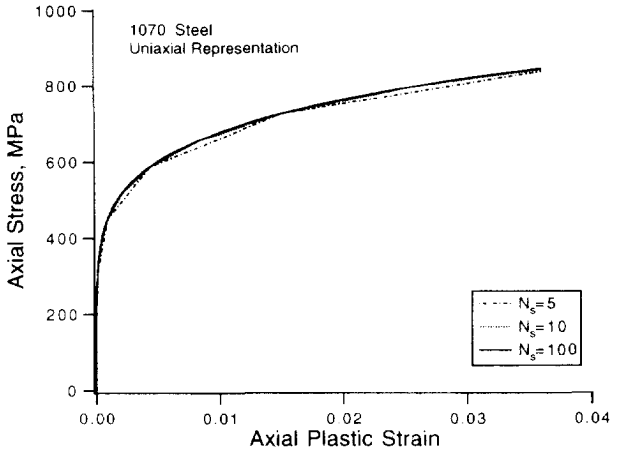

Fig. 13. Uniaxial representation for 1070 steel.

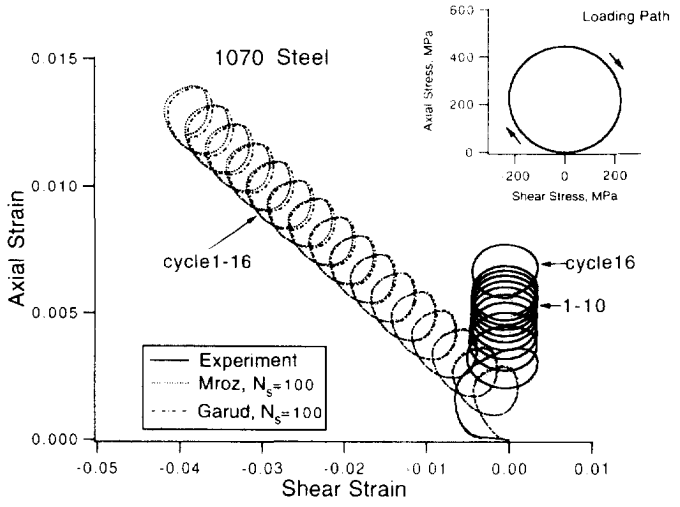

Fig. 14. Comparison of experimental ratchetting results and predictions by the Mroz and Garud models for a nonproportional axial–torsion loading path.

5. RATCHETTING PREDICTIONS WITH MULTIPLE SURFACE MODELS

5.1. *Nonproportional loading experiments under stress control*

The uniaxial representation of 1070 steel with multiple surfaces is depicted in Fig. 13. Similar to the 1045 steel, the amount of surface influence diminishes when N_s exceeds five. A comparison of experimental ratchetting results and predictions by the Mroz and Garud models for a nonproportional axial–torsion loading path is presented in Fig. 14. The stress-controlled "ellipse" shaped axial–torsion loading path was conducted on a 1070 steel tubular specimen (Jiang, 1993). With tensile axial mean stress, there is progressive strain extension in the axial direction. The experimental ratchetting in the shear direction for this loading path is minimal. The material displays long term ratchetting rate decay. In the simulations, 4000 incremental steps are employed for each loading cycle and the number of surfaces used in the models is 100. The material constants for the models are not important for the points of discussion but can be found elsewhere (Jiang, 1993). From Fig. 14 we find that the two multiple surface models are able to produce constant ratchetting rate for the "ellipse" shaped loading path in both axial and shear directions, but predicted results are very different from the experimental observations. The ratchetting rate predicted by the Mroz and Garud models for the nonproportional loading is constant and exhibits no decay. More notably, the models predict large shear ratchetting while the experiment displays practically no ratchetting in this direction. The two models predict virtually identical results.

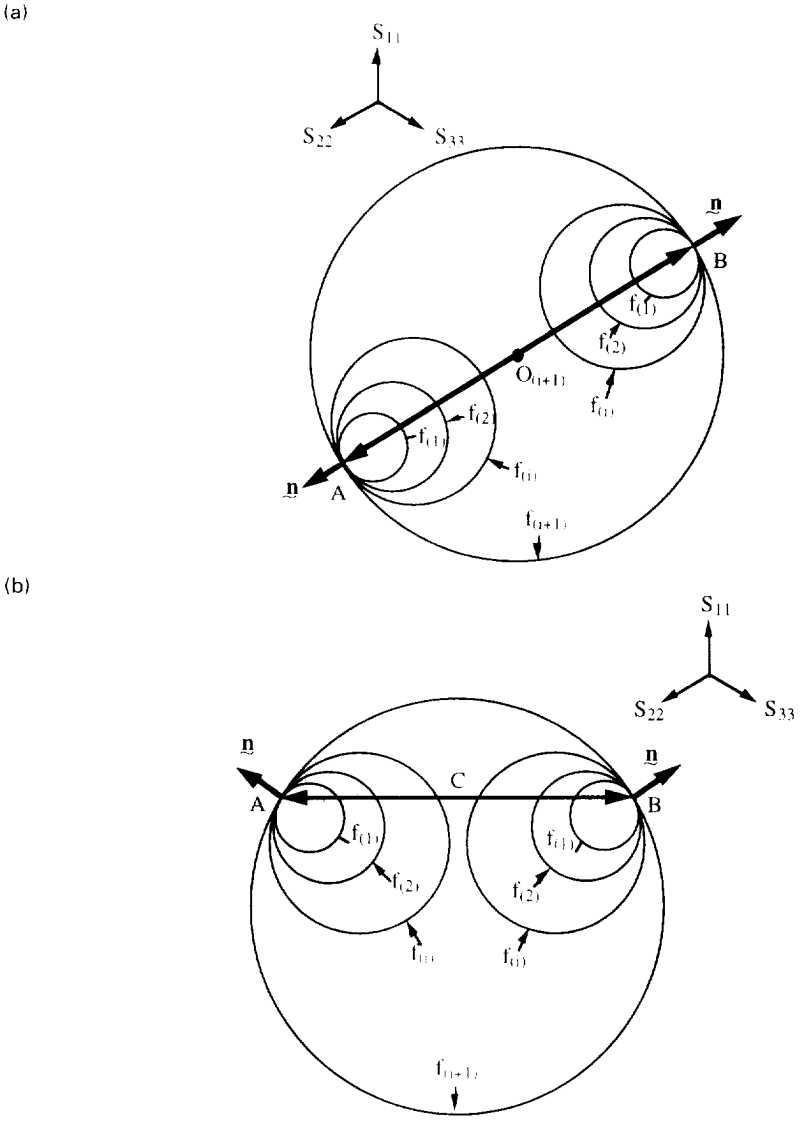

Fig. 15. Surface translation for proportional and nonproportional loading according to the Mroz model: (a) surface translation for proportional loading; (b) surface translation for nonproportional loading.

5.2. *Explanation of ratchetting under the nonproportional loading case*

The finding that a multiple surface model does not predict ratchetting for proportional loading but predicts ratchetting for nonproportional loading can be explained as follows. Rewriting the flow rule, eqn (2), in the indicial form leads to

$$\mathrm{d}\varepsilon^{p}_{mn} = \frac{1}{h}\langle \mathrm{d}S_{kl} n_{kl}\rangle n_{mn}. \tag{11}$$

Ratchetting rate is the amount of strain progression during a loading cycle. Presenting this expression mathematically, we have,

$$\frac{\mathrm{d}\varepsilon^{p}_{mn}}{\mathrm{d}N} = \int_{\text{cycle}} \mathrm{d}\varepsilon^{p}_{mn} = \int_{\text{cycle}} \frac{1}{h}\langle \mathrm{d}S_{kl} n_{kl}\rangle n_{mn}. \tag{12}$$

where $\mathrm{d}\varepsilon^{p}_{mn}/\mathrm{d}N$ is the ratchetting rate in the mn direction.

Referring to Fig. 15a, a proportional loading path is represented by $AO_{(i+1)}BO_{(i+1)}A$. Assume that for this loading path the first 1–ith surface translates while the other surfaces

larger than i will not move. Because of proportional loading, the plastic modulus function, h, and the value of the inner product $\mathrm{d}S_{kl}n_{kl}$ will vary symmetrically with respect to the $(i+1)$th surface center, $O_{(i+1)}$, and are always non-negative. The value of a normal component n_{ij} will vary symmetrically with respect to the fixed point, $O_{(i+1)}$, but the sign of the normal component n_{ij} will change. As a result, the integral in right-hand side of eqn (12) is always zero, hence no ratchetting is predicted in any direction.

We present Fig. 15b to study the nonproportional loading behavior. The loading path, ACBCA, consists of a static stress in the 11 direction and fully reversed stress components in the other direction. The ratchetting rate in the 11 direction can be expressed as

$$\frac{\mathrm{d}\varepsilon_{11}^{p}}{\mathrm{d}N} = \int_{ACBCA} \frac{1}{h} \langle \mathrm{d}S_{kl}n_{kl} \rangle n_{11}. \tag{13}$$

Again, h and $\mathrm{d}S_{kl}n_{kl}$ are non-negative and are symmetric with respect to the middle point C between A and B. For this loading path, the variation of the normal component n_{11} is symmetric with respect to the same middle point C but does not change its sign for a loading cycle. As a result, the integral of eqn (13) is a non-zero value. Considering cyclically stable material properties, the variations of h and $\mathrm{d}S_{kl}n_{kl}$, and n_{11} do not depend on the number of cycles. Therefore, a constant ratchetting rate is predicted. This explains the constant ratchetting predicted by the Mroz and Garud multiple surface models for the nonproportional loading reported by Garud (1991) and Hassan *et al.* (1992). Garud (1991) demonstrated the ability of his model to predict ratchetting for a nonproportional loading path of steady internal pressure with superimposed cyclic torsion. Hassan *et al.* (1992) used the Mroz model to simulate a loading consisting of static internal pressure and axial strain-symmetric cycling.

6. CONCLUSIONS

(1) The number of surfaces in the multiple surface models of Mroz and Garud has a significant influence on the translation direction of the yield surface and, hence the stress–strain predictions. This number of surface employed can in fact be viewed as a controlling parameter or model coefficient, but a quantitative relationship between this parameter and the predicted results is yet to be formulated.

(2) When the loading increment is infinitesimal, no intersection of surfaces will occur for the Mroz and Garud multiple surface models. Intersection of surfaces may occur when using the Mroz model for finite loading increment but will not occur when using the Garud model.

(3) For general nonproportional loading, the multiple surface models can predict ratchetting. However, the predicted ratchetting rates generally differ from the experimental observations.

Acknowledgements—The authors would like to acknowledge the financial support from the Association of American Railroads, Technical Center, Chicago, Illinois with Dr Dan Stone as monitor. The cooperation of Roger Steele, Gerald Moyar and Michael Fee is greatly appreciated.

REFERENCES

Armstrong, P. J. and Frederick, C. O. (1966). A mathematical representation of the multiaxial Bauschinger effect. Report RD B N 731, Central Electricity Generating Board.

Barkey, M. E., Socie, D. F. and Hsia, J. K. (1994). A yield surface approach to the estimation of notch strains for proportional and nonproportional cyclic loading. *J. Engng Mater. Technol. (ASME)* **116**, 173–180.

Benallal, A. and Marquis, D. (1987). Constitutive equations for nonproportional elastioviscoplasticity. *J. Engng Mater. Technol. (ASME)* **109**, 326–336.

Bruhns, O. T. and Pape, A. (1989). A three surface model in nonproportional cyclic plasticity. In: *Proc. Int. Conf. on Constitutive Laws for Engineering Materials* Chongqing, China (Edited by J. Fan and S. Murakami), Vol. 2, pp. 703–708. Pergamon Press, Oxford.

Chaboche, J. L. (1989). A new kinematic hardening rule with discrete memory surfaces. *Rech. Aérosp.* **4**, 49–69.

Chaboche, J. L., Dang Van, K. and Cordier, G. (1979). Modelization of the strain memory effect on the cyclic hardening of 316 stainless steel. SMiRT-5, Division L, Berlin, L11/3.

Chu, C. C. (1984). A three dimensional model of anistropic hardening in metals and its applications to the analysis of sheet metal formability. *J. Mech. Phys. Solids* **32**, 197–212.

Dafalias, Y. F. (1981). A novel bounding surface constitutive law for the monotonic and cyclic hardening response of metals. SMiRT-6, L3/4.

Dafalias, Y. F. and Popov, E. P. (1975). A model of nonlinearly hardening materials for complex loading. *Acta Mech.* **21**, 173–192.

Drucker, D. C. (1988). Conventional and unconventional plastic response and representation. *Appl. Mech. Rev.* **41**, 151–167.

Fatemi, A. (1985). Fatigue and deformation under proportional and nonproportional biaxial loading. Ph.D. dissertation, Mechanical Engineering, The University of Iowa.

Garud, Y. S. (1981). A new approach to the evaluation of fatigue under multiaxial loadings. *J. Engng Mater. Technol. (ASME)* **103**, 118–125.

Garud, Y. S. (1991). Notes on cyclic dependent ratchetting under multiaxial loads including Bauschinger effect and non-linear strain hardening. In *SMiRT-11* (Edited by H. Shibata) Vol. L, L23/1, pp. 511–518, Tokyo, Japan.

Hashiguchi, K. (1988). A mathematical modification of two surface model formulation in plasticity. *Int. J. Solids Structures* **24**, 987–1001.

Hashiguchi, K. (1993). Mechanical requirements and structures of cyclic plasticity models. *Int. J. Plast.* **9**, 721–748.

Hassan, T., Corona, E., and Kyriakides, S. (1992). Ratchetting in cyclic plasticity, part II: multiaxial behavior. *Int. J. Plast.* **8**, 117–146.

Howell, M., Hahn, G. T., Rubin, C. A. and McDowell, D. L. (1993). Finite element analysis of rolling contact for non-linear kinematic hardening bearing steel. Submitted to *J. Tribol. (ASME)*.

Hunsaker, B., Jr, Vaughan, D. K. and Stricklin, J. A. (1976). A comparison of the capability of four hardening rules to predict a material's plastic behavior. *J. Pressure Vessel Technol. (ASME)* **98**, 66–74.

Iwan, W. D. (1967). On a class of models for the yielding behaviour of continuous and composite systems. *J. Appl. Mech. (ASME)* **34**, 612–617.

Jiang, Y. (1993). Cyclic plasticity with an emphasis on ratchetting. Ph.D. dissertation, Department of Mechanical Engineering, University of Illinois at Urbana-Champaign.

Jiang, Y. and Sehitoglu, H. (1994). Cyclic ratchetting of 1070 steel under multiaxial stress states. *Int. J. Plast.* **10**, 579–608.

Kottgen, V. B. and Seeger, T. (1993). A Masing type integration of the Mroz model for some non-proportional stress-controlled paths. Submitted to *J. Engng Mater. Technol. (ASME)*.

Krieg, R. D. (1975). A practical two surface plasticity theory. *J. Appl. Mech. (ASME)* **42**, 641–646.

Lamba, H. S. and Sidebottom, O. M. (1978). Cyclic plasticity for nonproportional paths, part II: comparison with predictions of three incremental plasticity models. *J. Engng Mater. Technol. (ASME)* **100**, 104–111.

McDowell, D. L. (1985). A two surface model for transient nonproportional cyclic plasticity, part I: development of appropriate equations. *J. Appl. Mech. (ASME)* **52**, 298–302.

McDowell, D. L. (1989). Evaluation of intersection conditions for two-surface plasticity theory. *Int. J. Plast.* **5**, 29–50.

McDowell, D. L. (1992). Description of nonproportional cyclic ratchetting behavior. *Proc. MECAMAT'92, Int. Sem. on Multiaxial Plasticity*, Cachan, France, 1–4 September.

Mroz, Z. (1967). On the description of anisotropic workhardening. *J. Mech. Phys. Solids* **15**, 163–175.

Mroz, Z. (1969). An attempt to describe the behavior of metals under cyclic loads using a more general workhardening model. *Acta Mech.* **7**, 199–212.

Mroz, Z. (1981). On generalized kinematic hardening rule with memory of maximum prestress. *J. De Mech. Appl.* **5**, 241–260.

Mroz, Z. (1983). Hardening and degradation rules for metals under monotonic and cyclic loading. *J. Engng Mater. Technol. (ASME)* **105**, 113–118.

Ohno, N. and Wang, J. D. (1991). Transformation of a nonlinear kinematic hardening rule to a multisurface form under isothermal and nonisothermal conditions. *Int. J. Plast.* **7**, 879–891.

Ohno, N. and Wang, J. D. (1993). Kinematic hardening rules with critical state of dynamic recovery: part I—formulation and basic features for ratchetting behavior. *Int. J. Plast.* **9**, 375–390.

Prager, W. (1955). The theory of plasticity: a survey of recent achievements. *Proc. Inst. Mech. Engrs (Lond.)* **169**, 41–57.

Tipton, S. M. (1985). Fatigue behavior under multiaxial loading in the presence of a notch: methodologies for the prediction of life to crack initiation and life spent in crack propagation. Ph.D. dissertation, Mechanical Engineering Department, Stanford University, CA.

Tseng, N. T. and Lee, G. C. (1983). Simple plasticity model of the two-surface type. *J. Engng Mech. (ASCE)* **109**, 795–810.

Ziegler, H. (1959). A modification of Prager's hardening rule. *Q. Appl. Mech.* **17**, 55–65.